Article

Not peer-reviewed version

Enhancing the Durability of Reinforced Concrete Structures Using Carbonation-Inhibiting and CO2-Absorbing Microcapsules

Rei Yoshikawa , Ryusei Kondo , Koji Ishimaru , Shiro Kiyoyama , Kentaro Yasui *

Posted Date: 2 February 2026

doi: 10.20944/preprints202602.0063.v1

Keywords: carbonation; microcapsule; amine compounds; alkali-supplying; CO2 absorption; compressive strength

Preprints.org (www.preprints.org) | NOT PEER-REVIEWED | Posted: 2 February 2026 doi:10.20944/preprints202602.0063.v1

Article

Enhancing the Durability of Reinforced Concrete Structures Using Carbonation-Inhibiting and CO_2-Absorbing Microcapsules

Rei Yoshikawa [1], Ryusei Kondo [2], Koji Ishimaru [2], Shiro Kiyoyama [3] and Kentaro Yasui [4,*]

[1] Advanced Civil Engineering, National Institute of Technology, Kagoshima College, 1460-1 Shinko, Hayato-cho, Kirishima 899-5193, Japan
[2] Kyokuto Kowa Corporation, 2-6-31, Hikarimachi, Higashi-ku, Hiroshima 732-0052, Japan
[3] National Institute of Technology, Miyakonojo College, 473-1 Yoshio-cho, Miyakonojo, Miyazaki 885-8567, Japan
[4] Department of Urban Environmental Design and Engineering, National Institute of Technology, Kagoshima College, 1460-1 Shinko, Hayato-cho, Kirishima, Kagoshima 899-5193, Japan
* Correspondence: yasui@kagoshima-ct.ac.jp

Abstract

Carbonation degrades reinforced concrete structures and reduces their service life, and it raises environmental concerns. Moreover, the cement industry faces increasing pressure to mitigate CO_2 emissions. Therefore, this study developed a functional mortar incorporating microcapsule (MC) technology to suppress carbonation and enhance CO_2 absorption. Two types of MCs were prepared: alkali-supplying MCs for carbonation resistance and CO_2-absorbing MCs for carbon fixation. Mortars incorporating these MCs were evaluated using compressive strength tests, accelerated carbonation tests, and CO_2 absorption measurements. The alkali-supplying MCs effectively suppressed carbonation, particularly at a dosage of 10%. However, the compressive strength decreased owing to the low strength and density of the MCs. The CO_2-absorbing MCs significantly increased the CO_2 uptake, particularly when impregnated with amines such as trioctylamine. However, they did not suppress carbonation, and their absorption capacities decreased over time. MCs without amine impregnation absorbed CO_2, although they did not affect the carbonation depth owing to the absence of reactive components. These findings demonstrate the potential of MC-based mortars to improve the durability of concrete and promote carbon management. The use of cementitious materials with CO_2-absorbing and protective functions is a promising approach for sustainable construction and long-term infrastructure resilience.

Keywords: carbonation; microcapsule; amine compounds; alkali-supplying; CO_2 absorption; compressive strength

---

1. Introduction

In recent years, there has been a strong demand for extending the service life of reinforced concrete structures to reduce maintenance costs and environmental impact. However, degradation phenomena such as carbonation, salt damage, and alkali-silica reaction (ASR) make it difficult to achieve these goals. Among the preventive measures employed to counter carbonation, the effective approaches include reducing the water–cement ratio to densify concrete and coating surfaces with waterproofing materials or paints [1]. However, these methods require a high cement content and periodic maintenance.

Technologies that minimize CO_2 emissions from cement production are important for further reducing its environmental impact. However, the introduction of substitute materials and new processes is challenging both with respect to their cost and availability, and no material comparable to cement has emerged. Therefore, there has been increased focus on technologies that reduce or sequester CO_2 both before and after concrete production.

Amine compounds, known for their CO_2-absorbing properties, have attracted considerable attention. Typical examples include monoethanolamine (MEA), diethanolamine (DEA), triethanolamine (TEA), triisopropanolamine (TIPA), and trioctylamine (TOA) (Table 1) [2–6]. These alkanolamines differ in the number of hydrogen atoms in ammonia that are replaced by hydrocarbon groups [7].

Table 1. Classification of amine utilization in previous studies [2–6].

Amine	Category	Usage example
MEA	Primary amine	Carbonation promotion
DEA	Secondary amine	Early strength enhancer
TEA	Tertiary amine	Set accelerator
TIPA	Tertiary amine	Long-term strength enhancer
TOA	Tertiary amine	No reported usage in cement

There have been many applications of amines in concrete. The use of MEA and DEA in cementitious materials, including the use of post-CO_2-capture amine solutions for carbonation [2,8,9], and their effective inclusion as accelerators in sprayed concrete to improve early strength and hardening time have been investigated [3,10]. TEA, a widely used cement accelerator, enhances the initial strength of hardened cement by promoting setting. However, it has been reported to cause a slight decrease in long-term strength [4,5,11]. TIPA is also used as a grinding aid to prevent electrostatic agglomeration of particles during cement grinding and as a hardening accelerator similar to TEA [12]. Although the early strength of cementitious materials is comparable to that of those containing TEA, they show superior long-term strength owing to the formation of denser hydration products such as calcium silicate hydrate (C-S-H) [6,13]. TOA has limited applications in the concrete field, where it is still largely at the research stage. By contrast, its applications in the chemical and environmental fields include solvent extraction and wastewater treatment [14–17].

However, adding large amounts of these amine compounds to concrete is known to adversely affect strength development. Therefore, this study aimed to develop modified concrete by encapsulating amine compounds within microcapsules (MCs). This approach protects the amines from the concrete during mixing and allows their functional properties to be activated after hardening.

MCs are micrometer-sized capsules, and the process of encapsulating a core substance within a shell material to form MCs is termed MC encapsulation [18]. This technology has been widely applied in the food, medical, and environmental sectors. In the food sector, MCs are used to produce foods with functional claims and foods for specified health uses, which has been driven by health concerns arising from severe acute respiratory syndrome (SARS), Middle East respiratory syndrome (MERS), and coronavirus disease 2019 (COVID-19), as well as societal factors such as an aging population [19,20]. In the medical field, they serve as a useful drug delivery system. For example, they can efficiently deliver live probiotics to the large intestine [21]. MC encapsulation enables core isolation, protection, preservation, and release; solidification of liquid or gaseous cores into solid particles; and core density adjustment. By leveraging these characteristics in the field of concrete, functionality may be maintained long-term without requiring post-production maintenance. However, as the function of MCs varies with the preparation method, it is necessary to tailor MCs according to the intended purpose.

Previous studies on MC technology have mainly focused on enhancing the self-healing capability and durability of concrete. Specifically, polymeric materials such as urea-formaldehyde resin and sodium silicate have been used as shell materials for MCs, where they have demonstrated certain effectiveness in crack repair and the improvement of mechanical properties [22–24]. However, the use of MC technology to improve environmental durability—such as carbonation resistance and

CO_2 uptake—remains limited, and its effectiveness in these contexts has not been investigated sufficiently.

Therefore, this study aimed to develop a method to extend the service life and enhance the sustainability of reinforced concrete (RC) structures using concrete mixed with MCs. A functional mortar containing MCs was prepared, and its physical properties and functionality were evaluated. For MC preparation, an alkali-supplying type MC targeting concrete carbonation inhibition was first prepared. However, this MC was low in density, leading to a floating phenomenon within the fresh mortar, indicating a need for improving the preparation method. Furthermore, considering the recent advances in research on technologies to fix CO_2 within concrete, a CO_2-absorbing-type MC was also prepared to broaden the application scope of MCs.

This study is unprecedented in that it prepares MCs with alkaline-releasing and CO_2-absorptive properties, incorporates them into mortar, and systematically evaluates both the physical properties and functional performance of the resulting materials, particularly in terms of the carbonation resistance and CO_2 uptake. This research is expected to contribute to the development of new construction materials that enhance the longevity of RC structures and reduce environmental impact.

The remainder of this paper is organized as follows. Section 2 describes the preparation methods for functional mortars using two types of MCs and the test methods for evaluating their corresponding physical properties and functionalities. Section 3 presents the results of various performance evaluation tests conducted on the mortars containing alkali-supplying and CO_2-absorbing MCs. Section 4 summarizes the findings and outlines future research.

2. Materials and Methods

2.1. Preparation and Experimental Methods for Carbonation-Resistant Mortar

2.1.1. Preparation of Alkali-Supplying MCs

Figure 1 shows a scanning electron microscopy (SEM) image of the MC used in this study, Figure 2 shows a schematic cross-section of the MC, Figure 3 shows the preparation flow, and Figure 4 shows the MC regulating device. The MC was prepared via the in-liquid drying method using an emulsion composed of a solid phase (S)/organic phase (O)/external aqueous phase (W) as the starting material [25,26]. The preparation method is shown below.

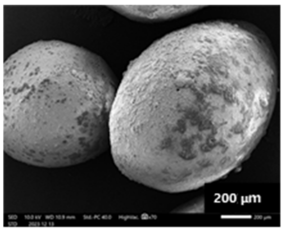

Figure 1. SEM image of microcapsule (MC) particles.

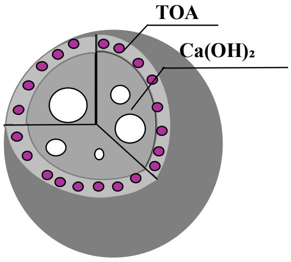

Figure 2. Schematic of MC cross-section.

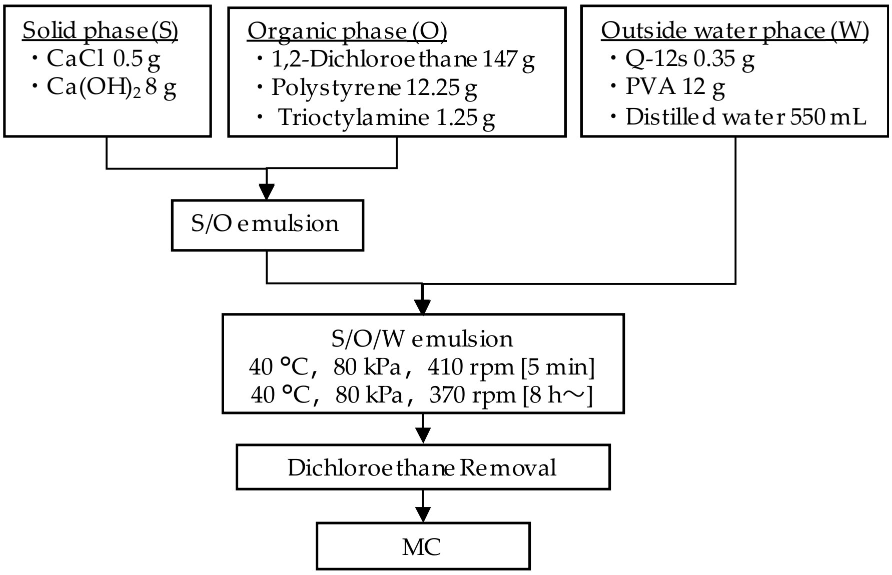

Figure 3. Process flow of liquid drying.

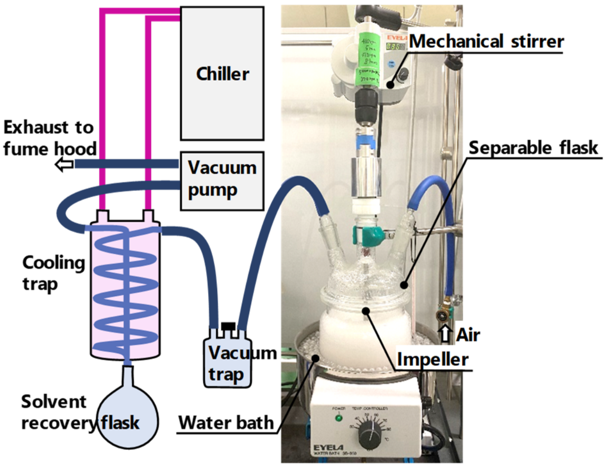

Figure 4. MC regulating device.

1. The solid phase containing Ca(OH)$_2$ as an alkaline source and the organic phase containing TOA were stirred at 3000 rpm for 24 h using a homogenizer (CM-100S, AS ONE Corporation, Osaka, Japan) to prepare the S/O emulsion.
2. A 1 L separable flask was placed in a water bath (SB-350, Tokyo Rikakikai Co., Ltd., Bunkyo-ku, Japan) maintained at 40 °C, and the external aqueous phase was stirred using a stirrer (ZZ-1010, Tokyo Rikakikai Co., Ltd., Bunkyo-ku, Japan) inside the flask.
3. While continuing to stir, the internal pressure of the flask was reduced to 80 kPa using a vacuum pump (DTC-41, ULVAC, Inc., Chigasaki, Japan), and the S/O emulsion was added under this reduced-pressure condition.
4. Under the same conditions, the flask was stirred at 410 rpm for 5 min, followed by stirring at 370 rpm for 8 h to prepare the S/O/W emulsion. Volatile gases, including dichloroethane, generated during this process were extracted using a vacuum pump and then condensed and recovered using a cooling trap and a chiller (CCA-1112A, Tokyo Rikakikai Co., Ltd., Bunkyo-ku, Japan).
5. The external aqueous phase was removed by filtration and washing, and the MC was obtained by drying in an oven (DSN-114, Isuzu Manufacturing Co., Ltd., Sanjo, Japan) at 70 °C for 24 h.

The in-liquid drying method has the advantage that the amount of the shell material directly reflects the membrane thickness of the MC, allowing for easy control of the film thickness [27].

Furthermore, because the pore size of the MCs prepared using this method can be varied by changing the solvent type and removal rate, the core-release rate can be controlled. The resulting MCs consist of a polystyrene shell encapsulating $Ca(OH)_2$ as the core, with their particle size ranging from 300 to 1200 μm (Figure 1).

The mechanism underlying the alkaline compound supply via the MC is as follows. The MC has a structure in which molecular-level micropores present in the polystyrene shell, which are sealed with TOA (Figure 2). When the pH around the MC decreases below 10, TOA forms a hydrochloride salt and becomes more hydrophilic, thus promoting the release of $Ca(OH)_2$, which is the alkaline source retained in the MC core. As a result, the pH around the MC increases to 12–13, and TOA returns to its hydrophobic state, which suppresses the diffusion of $Ca(OH)_2$. Thus, using the reversible change in the hydrophilicity and hydrophobicity of TOA, the release of $Ca(OH)_2$ is controlled until it is depleted.

2.1.2. Verification of pH Responsiveness of Alkali-Supplying MC

To confirm the pH responsiveness of the alkaline-supplying MC, a suspension was prepared by dispersing 1.0 g of the MC in 50 mL of distilled water, and measurements were performed using a pH meter. To this suspension, 1 mol/L hydrochloric acid was added dropwise in 200 μL increments, and the pH change was recorded after each addition. A temporary reduction in the pH was observed immediately after each addition of hydrochloric acid. However, the pH subsequently recovered to an alkaline state as hydroxide ions were supplied from the MC. Therefore, the pH at the point of stabilization was adopted as the measured value, and the maintainable pH range of the MC was evaluated accordingly.

2.1.3. Preparation of Alkaline-Supplying Mortar

Table 2 shows the mix design for the alkali-supplying mortar prepared in this study. The target compressive strength of the mortar was set to 21 N/mm², as this strength class is commonly used in concrete structures. As the preparation procedure, ordinary Portland cement (OPC) and crushed sand were dry-mixed at 64 rpm for 1 min, followed by the addition of water while mixing in a mortar mixer (KC-8, Kansai Kiki Co., Ltd., Amagasaki, Japan) at 107 rpm for 2 min. Subsequently, the MC was added at 0, 1, 5, and 10% of mortar volume, followed by mixing at 107 rpm for 30 s. The resulting mortar was filled into cylindrical molds (inner diameter: 50 mm, height: 100 mm) and sealed for curing at a temperature of 20 °C for 28 d.

Table 2. Mix proportions of the carbonation-resistant mortar samples.

W/C (%)	kg/m³			g/m³
	Water	Cement	Sand	MC
65	220	338	1756	14.1

*MCs added externally at 1 vol% of the total mortar.

2.1.4. Evaluation Test for Alkali-Supplying Mortar

Compressive strength tests were conducted on the mortar specimens cured for 7 and 28 d in accordance with Japanese Industrial Standard (JIS) A 1108 [28]. Accelerated carbonation tests were also performed in accordance with JIS A 1153 [29] under the following conditions: 20 °C, 60% relative humidity, and 5% CO_2 concentration.

To perform the accelerated carbonation test, the exposed surface was set as the casting surface of the mortar, while the other surfaces were sealed with an epoxy resin (Resiguard WP-NS, Dainippon Toryo Co., Ltd., Osaka, Japan). The accelerated carbonation periods were set to 4, 12, and 24 w. After the carbonation period, a 1% phenolphthalein solution was sprayed onto the fracture surfaces of the test specimens, and coloration was observed. The carbonation depth was determined by measuring the depth of the colorless region from the exposed surface at 10 locations using digital calipers and calculating the average value.

2.2. Preparation and Experimental Methods for CO_2-Absorbing Mortar

2.2.1. Preparation of CO_2-Absorbing MCs

Figure 5 shows the SEM image of the CO_2-absorbing-type MC used in this study, Figure 6 shows a schematic cross-section of the MC, and Figure 7 shows the preparation flow. The MC was prepared via a polymerization method using a solid phase (S)/organic phase (O)/external aqueous phase (W) as the starting material [30]. The preparation method is shown below.

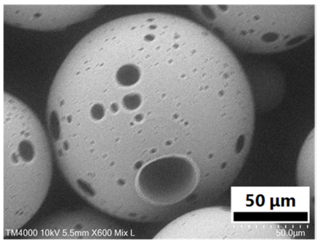

Figure 5. SEM image of the polymerization-derived MC particles.

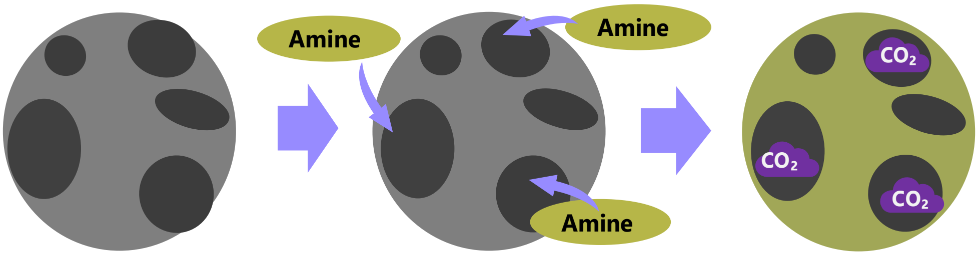

Figure 6. Schematic of the CO_2-absorbing MC formed by amine impregnation into the polymerized MC.

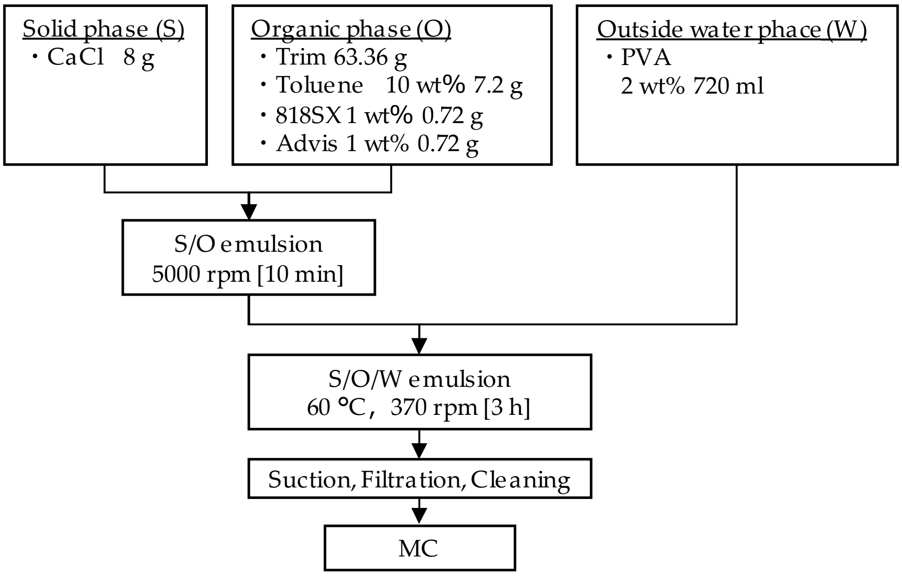

Figure 7. Process flow of the polymerization method.

1. The solid and organic phases were stirred using a homogenizer at 5000 rpm for 10 min to prepare the S/O emulsion.

2. Using the preparation apparatus shown in Figure 4, the external aqueous phase was placed in a separable flask within a water bath set to 55 °C and stirred at 370 rpm, followed by the addition of the S/O emulsion.
3. Subsequently, stirring at 370 rpm for 3 h at 60 °C and atmospheric pressure yielded an S/O/W emulsion. During this process, because of the volatility and flammability of toluene present in the organic phase, all operations were conducted in a fume hood equipped with local exhaust ventilation.
4. The MC was obtained by suction filtration while washing with distilled water, followed by drying for 24 h in a drying oven set to 70 °C.

Compared to the liquid-phase drying method, the polymerization method enables MC preparation under high-temperature conditions without requiring vacuum, thus enabling large-scale production. Furthermore, as shown in Figure 5, a large number of pores were formed on the surface and inside the MCs, facilitating the preparation of porous MCs [31]. The particle size of the obtained MC was 100–130 μm.

Next, an impregnation treatment was performed to disperse and fix TOA onto the MC prepared by the polymerization method. Impregnation is a technique that allows liquids or agents to penetrate the fine gaps and pores within a material. Figure 8 shows the apparatus used for the MC impregnation process. Specifically, 10 g of MCs and 1 g of TOA were added to a 500 mL round-bottom flask, and an adequate amount of ethanol was added to ensure sufficient immersion. The flask was placed in a water bath attached to a rotary evaporator (REV202M, Yamato Scientific Co., Ltd., Chuo-ku, Japan), which was set to 30–40 °C. Under stirring at 80–100 rpm, the pressure was gradually reduced from 20 to 10 kPa in stages, avoiding boiling. This process achieved 10% TOA impregnation relative to the MC mass while vaporizing and recovering ethanol. Subsequently, the resulting TOA-impregnated MC (TOA-MC) was dried for 24 h in a drying oven at 70 °C.

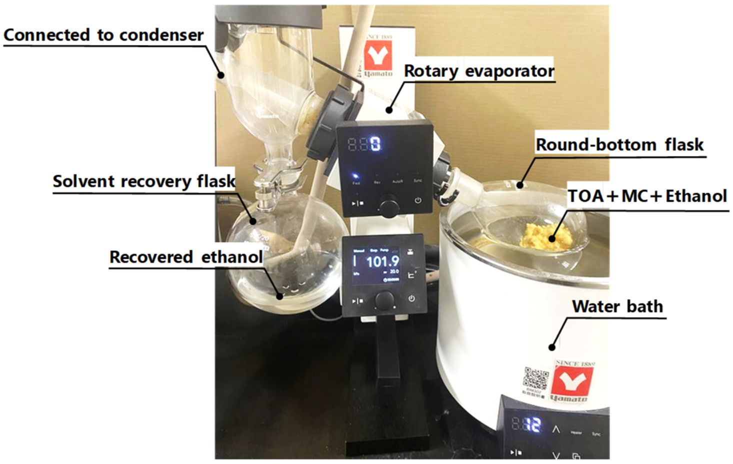

Figure 8. Apparatus used for the impregnation of the MC with amine compounds.

In addition to TOA, amine compounds reported to exhibit CO_2 absorption effects (DEA, TEA, and MEA) were considered for impregnation into the MCs [2,8,9,11,32,33]. However, in preliminary experiments, the mortar produced using the MC impregnated with these compounds did not develop strength; this was possibly because compounds like DEA are water soluble and leach into water during mortar mixing, failing to remain within the MC. Therefore, oil-soluble TOA, an oil-soluble amine, was selected. Impregnating MC with this compound resulted in the formation of a structure whose stability was retained within the mortar. The CO_2 absorption mechanism by amines involves the reaction where amines react with atmospheric CO_2 to form carbamates, thereby capturing CO_2 [34,35].

Although it is technically possible to incorporate TOA directly into the MC structure because of the organic phase in the polymerization process [36], there is a risk that amines could be lost along with distilled water during the filtration and washing steps.

This section describes the characteristics of encapsulation and impregnation during polymerization. Encapsulation via polymerization can prevent amine leakage and ensure stability and reusability, and it has been applied in studies focused on long-term use and recyclability [37,38]. However, issues such as the design of shells to prevent core leakage and the optimization of encapsulation efficiency have been reported [39]. By contrast, impregnation is a simple and cost-effective method that allows high-concentration amine loading, and it has been used in studies focused on capsule adsorption performance and economic efficiency [40–43]. However, the adsorption capacity tends to decrease with repeated CO_2 adsorption–desorption cycles, which makes it unsuitable for long-term use [44,45]. This study was focused on experimental process development; therefore, the impregnation method was used to ensure reliable fixation of the amine within the MCs [46].

2.2.2. Preparation of CO_2-Absorbing-MC-Added Mortar

Table 3 lists the specified mix proportions for the prepared mortar samples, and Table 4 lists the conditions for MC addition to the mortar. The test levels were plain (no MC), a mixed MC without impregnation, or a mixed MC with TOA impregnation (Table 4). The target compressive strength of the mortars was set to 30 N/mm² to accommodate the concrete structures. To evaluate the CO_2 absorption effect of the MCs, three types of mortars were prepared: plain mortar without MC addition (PL), mortar with MCs containing no TOA (MC-0), and mortar with MCs impregnated with 10% TOA by weight (MC-TOA).

Table 3. Mix proportions of the CO_2-absorbing mortar samples.

W/C	kg/m³			g/m³
(%)	Water	Cement	Sand	MC
55	208	378	1756	12.9

*MC is added externally at 5 vol% of the total mortar.

Table 4. Conditions for MC addition to the mortar.

No.	Name	MC present	MC contents	Addition rate (%)
1	PL	No	Not used	—
2	MC-0	Yes	No amine	5
3	MC-TOA	Yes	10% TOA added	5

The preparation procedure was as follows: First, OPC and water were mixed in a mortar mixer at 64 rpm for 1 min. Then, the MC equivalent to 5% of the mortar volume was added separately after initial mixing. Next, crushed sand was added and mixed at 107 rpm for 3 min. The resulting mortar was then filled into cylindrical molds with an inner diameter of 50 mm and a height of 100 mm, and sealed curing was conducted in a constant-temperature room at 20 °C for 28 d.

2.2.3. Evaluation Test of CO_2-Absorbing-MC-Added Mortar

On days 7 and 28 after curing, compression strength tests were conducted on the specimens in accordance with JIS A1108 [28]. For the accelerated CO_2 absorption test, three specimens for each condition aged for 1 d were dried in a drying oven at 40 °C for 24 h. As shown in Figure 9, the specimens were placed in a 12 L vacuum desiccator (VL-C, AS ONE Corporation, Osaka, Japan), where CO_2 was forcibly supplied to accelerate its absorption. CO_2 gas was periodically injected to maintain a CO_2 concentration of ~5% in the desiccator, and changes in the CO_2 concentration inside the desiccator were measured using a CO_2 concentration meter (E31-6979-10, Narika Corporation, Bunkyo-ku, Japan).

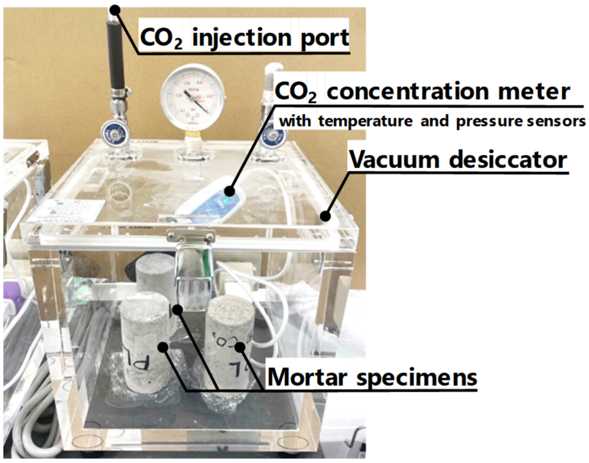

Figure 9. CO_2 absorption test apparatus.

For the test, an epoxy resin (Bond Quick Mender, Konishi Co., Ltd., Osaka, Japan) was applied to the bottom surface of the cylindrical specimens, leaving the remaining surfaces exposed. The CO_2 absorption periods were set at 20 weeks. Specimens were split at 4, 12, and 20 weeks after the start of the test, phenolphthalein solution was sprayed onto the fracture surface to visualize the carbonation areas, and the carbonation depth was measured. Furthermore, the CO_2 absorption amount in the carbonation area was measured at 20 weeks in accordance with JIS Z 2615 [47].

3. Results

3.1. Performance of Mortar Containing Alkali-Supplying MC

3.1.1. Verification of pH Responsiveness of Alkali-Supplying MC

Figure 10 shows the pH change observed when hydrochloric acid was added dropwise to the suspension with the dispersed MC containing distilled water. Immediately after hydrochloric acid addition, the pH stabilized at ~12.5. Subsequently, the pH decreased with the continued addition of hydrochloric acid, reaching a temporary stable state around pH 8. Continuing the addition of hydrochloric acid caused the pH to drop sharply once the added volume exceeded 5200 μL, ultimately reaching a pH of less than 4. These behaviors suggest that $Ca(OH)_2$ contained in the MC dispersed in distilled water was gradually released. In particular, the temporary stabilization observed around pH 8 may be attributed to either a concurrence of the release rate of $Ca(OH)_2$ and the addition rate of HCl or the preferential release of $Ca(OH)_2$ located near the surface of the MC. In other words, the expected pH responsiveness around pH 10–11, which was anticipated based on the properties of TOA, was not observed.

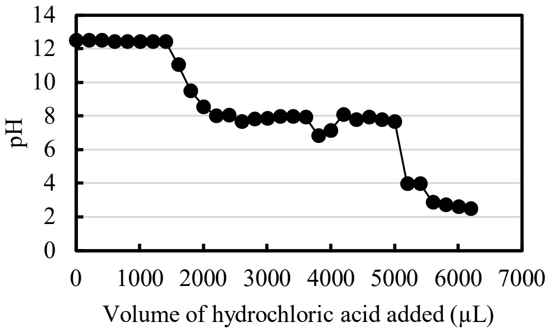

Figure 10. pH response of the MC containing distilled water to incremental hydrochloric acid addition.

3.1.2. Compressive Strength Test of Alkali-Supplying-MC-Added Mortar

Figure 11 shows the relationship between the MC addition rate and mortar compressive strength. The legend indicates the MC addition rate relative to the mortar volume. After 28 d, the compressive strength, the strength of the specimen decreased with increasing MC addition rate. The strength at 5% MC addition was only ~80% of that without MC addition.

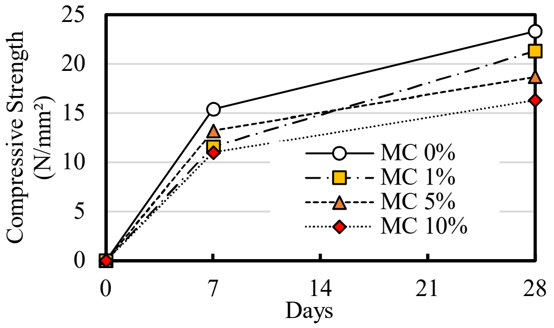

Figure 11. Relationship between the MC content and compressive strength.

The factors contributing to this strength reduction include the composition of the MC, which contains polystyrene, resulting in lower capsule strength than that of cement paste. Furthermore, adding the MC externally likely reduces the cement content per unit volume with an increase in the addition rate, consequently leading to strength reduction.

According to a report by Jawahar et al. [48], when a polyurethane-based MC was added to a cement mortar at 0.5–5.5% by cement weight, the addition of the MC at 4.5% (equivalent to ~1.0% by volume in this study) increased the compressive strength by 33.88% owing to secondary hydration reactions involving sodium silicate. Conversely, when the MC was added at 5.5% (equivalent to 1.3% in this study), the strength decreased by 25.31% owing to compromised structural integrity.

This strength reduction was attributed to the potential degradation of structural integrity caused by increased porosity and weakened interfaces, consistent with the trends observed in this study.

3.1.3. Accelerated Carbonation Test of Alkali-Supplying-MC-Added Mortar

Figure 12 shows the relationship between the MC addition rate and carbonation depth. Here, error bars represent the mean ± 2× standard deviation. Focusing on week 4 after the accelerated carbonation initiation, the carbonation depth of the mortar with 10% MC addition was 0.3 mm, whereas carbonation progressed to 2.4 mm for the mortar without the MC sample. This trend was similarly confirmed at 12 and 24 weeks. At week 24, the carbonation depth for the 10%-MC-added mortar was 2.3 mm, whereas carbonation progressed to 4.3 mm for the mortar without the MC. These results indicate that increasing the MC addition rate reduces the carbonation depth from the exposed surface, thereby suppressing carbonation progression. However, based on the results shown in Figure 10, it is highly likely that the suppression of carbonation was due to the release of $Ca(OH)_2$ located near the surface of the MC, rather than the pH responsiveness of TOA.

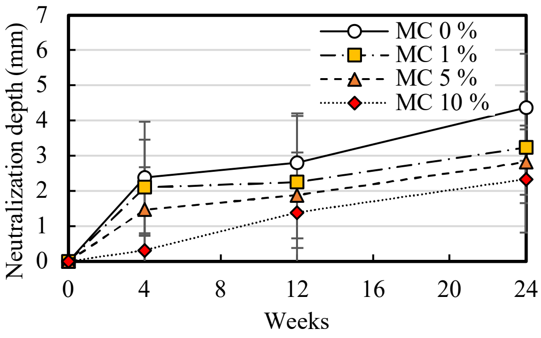

Figure 12. Relationship between the MC content and carbonation depth.

Table 5 shows the cross-sectional photographs of the specimens taken during carbonation depth measurements. As shown in Figure 12, the differences in the MC addition rate caused variations in the carbonation depth. The photographs in the table show colorless regions in the specimen cross-sections. This is likely due to a reduced cement content per unit volume caused by the MC addition, which reduced the compactness. Consequently, capillary voids may have formed at the casting (exposed) surface, potentially causing localized carbonation. The large error bars for the carbonation depth of the mortars with 1% and 5% MC addition are considered to be due to variations in the presence and extent of the colorless regions, which caused fluctuations in the measurement results.

Table 5. Cleaved specimens after the accelerated carbonation test.

MC addition rate	Promotion period		
	4 weeks	12 weeks	24 weeks
0%			
1%			
5%			
10%			

Based on these results, the characteristics of the alkali-supplying MC are summarized below. First, as the TOA used in this experiment released $Ca(OH)_2$ without exhibiting pH responsiveness, it is necessary to improve the MC structure so that it responds at a pH higher than 11, where reinforcement corrosion begins. Next, because the main material of the MC is polystyrene, the compressive strength of the mortar with the added MC decreased. In addition, the density of the polystyrene-based MC is low at 0.3 g/cm^3, making it prone to floating during mortar preparation and potentially causing difficulties in achieving uniform dispersion. Therefore, increasing the density of the MC is challenge that should be overcome in future studies.

3.2. Performance Evaluation of Mortar Containing CO_2-Absorbing MCs

3.2.1. Compressive Strength Test of CO_2-Absorbing-MC-Added Mortar

Figure 13 shows the change in the compressive strength over time for each MC content condition. The MC-TOA mortar achieved a target strength of 30 N/mm^2 at 28 d, which was only ~71% of the strength of PL without MC addition. Furthermore, the strength of MC-0, which did not incorporate TOA, was ~78% of that of PL.

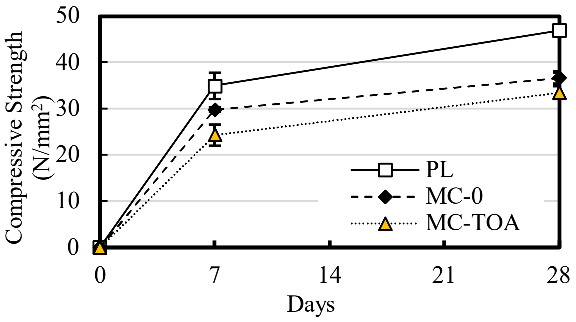

Figure 13. Relationship between the MC content and compressive strength.

This indicates that MC addition reduces mortar strength, and impregnating MC with TOA accentuates this reduction effect. The strength loss arises from the acrylic-based MC, whose strength is lower than that of cement paste. Because the MC is added to cement by external mixing, the amount of cement per unit volume is reduced, thereby lowering the mortar strength.

Furthermore, the strength difference observed between MC-0 and MC-TOA is presumed to be due to the influence of TOA, suggesting that a small amount of TOA may have leached from the MC and suppressed the strength development of the mortar. By contrast, Song et al. [12] demonstrated that adding tertiary amines such as Triisopropanolamine (TIPA), di-ethanol isopropanolamine (DEIPA), and methyl di-ethanolamine (MDEA) at 0.04% to fly ash cement can enhance early strength. This suggests that TOA has a different effect on strength development than other tertiary amines.

Furthermore, in preliminary experiments, the mortars containing the MC impregnated with the water-soluble amine compounds DEA, MEA, and TEA all failed to develop strength. Based on these results, in this study, the CO_2 absorption tests were conducted using MC-TOA, because it is the only amine-based sample among those prepared that showed strength development.

3.2.2. Accelerated CO_2 Absorption Test of CO_2-Absorbing-MC-Added Mortar

Figure 14 shows the time-dependent change in CO_2 absorption for each mortar specimen and test conditions during the accelerated CO_2 absorption tests, and Figure 15 shows the cumulative CO_2 absorption for each specimen after testing for 28, 56, 84, and 140 d.

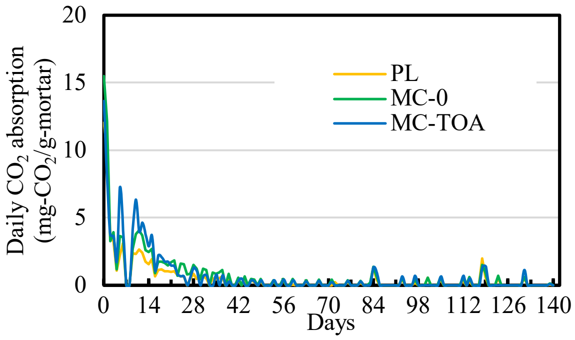

Figure 14. Daily CO_2 absorption per unit mass of the mortar.

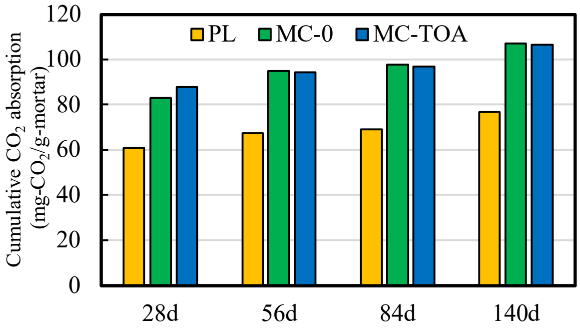

Figure 15. Cumulative CO2 absorption over 140 d.

Here, the absorption rate q_{CO_2} (mg) per gram of mortar, calculated from the CO2 concentration changes measured using the CO2 sensor, was calculated using Eqs. (1), (2), and (3).

$$\Delta n_{CO_2} = \left(\frac{C_1}{10^6} \cdot \frac{P_1 \cdot V}{R \cdot T_1}\right) - \left(\frac{C_2}{10^6} \cdot \frac{P_2 \cdot V}{R \cdot T_2}\right) \quad (1)$$

$$m_{CO_2} = \Delta n_{CO_2} \cdot M_{CO_2} \quad (2)$$

$$q_{CO_2} = \frac{m_{CO_2}}{m_{mortar}} \quad (3)$$

Here, Δn_{CO_2} is the reduction in CO2 moles due to concentration decrease (mol); C_1 is the CO2 concentration (ppm) inside the container immediately after CO2 injection; C_2 is the CO2 concentration (ppm) inside the container after CO2 absorption and immediately before the next CO2 injection; P_1 and P_2 are the pressures inside the container at the time when C_1 and C_2 were measured (Pa), respectively; V is the volume of the container (m^3) (12 L = 0.012 m^3); R is the gas constant (8.314 J/mol·K); T_1 and T_2 are the temperatures inside the container at the time when C_1 and C_2 were measured (°C), which were converted to absolute temperature using the equation T + 273.15 (K); m_{CO_2} is the amount of CO2 absorbed by the mortar (g); M_{CO_2} is the molar mass of CO2 (44.01 g/mol); and m_{mortar} is the total mass of the mortar that absorbed CO2 in the container (g).

The CO2 absorption decreased over time for all mortars. Note that CO2 absorption temporarily decreased on days 2, 7, and 8 after the start of the test owing to interruptions in the CO2 supply. This decrease is unrelated to the CO2 absorption performance of the mortars themselves.

For the cumulative CO2 absorption over 140 d, the mortar containing MC-TOA showed the high value at 107 mg-CO2/g-mortar, exhibiting ~1.4 times the absorption amount of the unmodified PL mortar (77 mg-CO2/g-mortar). Furthermore, the mortar containing the MC (MC-0) without TOA impregnation also absorbed more CO2 than the PL mortar. The absorption amount of the MC-0 mortar did not differ significantly from that of MC-TOA because of the possibility that the MC itself readily absorbs CO2, and that TOA is considered to have low CO2 absorption capacity.

Table 6 shows the cumulative CO2 absorption amounts obtained by analyzing the mortar collected at the start of the test and at 20 weeks (140 d). The CO2 uptake was 1.96–2.06 wt% at the start of the test and reached a maximum of 7.72 mass % in the MC-0 specimen by the end of the test. This value was of the same order of magnitude (7.72 mass % = 77.2 mg-CO2/g-mortar) as that of the CO2 absorption calculated from the measured CO2 concentration changes in the vacuum desiccator shown in Figure 5 (see also Figure 15) but showed particularly low values for MC-0 and MC-TOA. A comparison of the results from these test methods showed that, based on the calculated CO2 absorption over time, MC-TOA exhibited the highest absorption tendency among the three conditions in the initial stage. However, the analytical results at 140 d indicated that MC-TOA had the lowest absorption amount. This discrepancy is thought to stem from differences in the measurement principles. Furthermore, specimens exposed for 140 d in a 5% CO2 environment correspond to approximately 48 years of exposure in the natural environment (average CO2 concentration: 400 ppm). As this period is close to the typical design service life of 50 years for concrete structures, even if MC-TOA shows high absorption in the early stage, its long-term CO2 uptake performance is considered unsustainable.

Table 6. Cumulative CO_2 uptake of the mortar specimens at 20 weeks.

MC addition condition	Cumulative CO_2 uptake (mass %)	
	Start of the test	20 weeks
PL	1.97	7.40
MC-0	1.96	7.72
MC-TOA	2.06	7.18

Figure 16 shows the relationship between the MC addition rate and carbonation depth in the specimens after the accelerated CO_2 absorption tests. In the accelerated CO_2 absorption test, focusing on 4 weeks after exposure initiation, the carbonation depth of MC-TOA was 22 mm, which was greater than the approximately 17 mm observed for PL and MC-0. This is likely because MC-TOA absorbed a greater amount of CO_2. Figure 15 confirms that MC-0 absorbed more CO_2 than PL, possibly because MC-0 is porous, which allows easier CO_2 absorption compared to PL. However, no clear difference was observed between their carbonation depths.

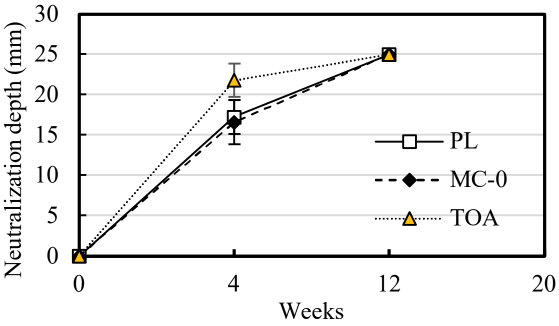

Figure 16. Relationship between the MC content and carbonation depth.

However, carbonation (pH reduction) proceeds through the reaction between calcium hydroxide ($Ca(OH)_2$), a cement hydration product, and CO_2. As MC-0 does not contain any substances inside the capsule that react with CO_2, the absorbed CO_2 does not contribute to the carbonation reaction. As a result, the carbonation depth of MC-0 is similar to that of PL.

At 12 weeks, the carbonation depth reached ~25 mm under all conditions. As shown in the cross-sectional photographs taken after the accelerated CO_2 absorption test (Table 7), the carbonation depth could be clearly determined at week 4, but by week 12, carbonation had progressed throughout the entire cross-section, making accurate measurement of the carbonation depth difficult. Therefore, the actual carbonation depth may have reached beyond 25 mm, making it difficult to evaluate the effect of TOA.

Table 7. Specimen cross-sections after the accelerated carbonation test.

MC addition rate	Exposure period		
	4 weeks	12 weeks	20 weeks
PL	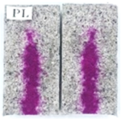		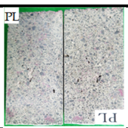
MC-0	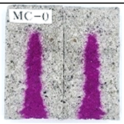	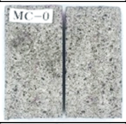	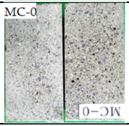
MC-TOA	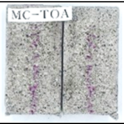	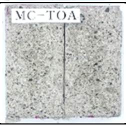	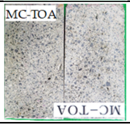

Thus, it was confirmed that the exposure method adopted in this experiment allows for effective evaluation of the carbonation depth only up to approximately 4 weeks after the start of exposure. Consequently, improvements to the test method are required to enable a quantitative evaluation of the carbonation depth over a long period, such as limiting the exposed surface to only the top surface of the cylindrical specimen.

Based on these results, the characteristics of the CO_2-absorbing MC are summarized below. First, as the TOA used in this experiment is an oil-soluble amine compound, its impact on compressive strength reduction when added to the mortar tends to be weaker than that observed when the water-soluble amine compounds are added to the MC. However, as strength reduction was still observed in relation to that in MC-0, it is necessary to investigate the methods for adjusting the MC to prevent amine leaching. Furthermore, even if leaching occurs, selecting amine compounds that contribute to strength development is crucial.

Second, the mortar containing the MC showed increased CO_2 absorption, with the addition of TOA-MC resulting in a further increase.

Moreover, the density of the acrylic MC is relatively high at 1.1 g/cm^3; thus, the acrylic MC potentially suppresses flotation during mortar preparation to a greater extent than the polystyrene MC.

Therefore, future improvements to MCs to balance structural performance and functionality, including the selection of oil-soluble amine compounds with high CO_2 absorption capacity, are important challenges.

4. Conclusions

In this study, functional mortars incorporating MC technology were developed to enhance the durability and sustainability of RC structures. First, a mortar mixed with alkali-supplying MCs was prepared to suppress carbonation, and a mortar mixed with CO_2-absorbing MCs was prepared to promote carbon fixation. The effects of these MCs on the mechanical properties and functional performance of mortars were evaluated. The key findings are summarized as follows:

1. Although clear pH responsiveness was not observed, a verification of the pH responsiveness of the alkali-supplying MCs suggested that $Ca(OH)_2$ was gradually released from the MC.
2. As the dosage of alkali-supplying MCs increased, the compressive strength decreased. This was attributed to the low strength of the polystyrene-based MCs and the reduction in the cement content due to external addition.
3. The suppression of carbonation depth became more pronounced with increasing MC dosage, and a significant reduction in carbonation was observed at 10% MC.
4. When 5% of the CO_2-absorbing MCs was added to the mortar, both the PL and MC-0 specimens reached the target strength of 30 N/mm^2 after 7 d, whereas the MC-TOA specimens achieved it after 28 d.
5. The incorporation of MCs (MC-0) enhanced the CO_2-absorption capacity of the mortar in relation to that of the plain mix (PL), and impregnation of the MCs with amines (MC-TOA) further increased their CO_2 uptake performance. Although MC-0 absorbed more CO_2 than PL, no difference in the carbonation depth was observed, likely because MC-0 did not contain reactive substances that contribute to carbonation reactions.
6. Under continuous CO_2 exposure, the CO_2 absorption capacity of the mortar gradually decreased over time.

This study confirmed that the initially developed alkali-supplying MCs effectively suppressed carbonation; however, their low density limited dispersion in mortar, restricting their applicability. Therefore, CO_2-absorbing MCs were developed by modifying the fabrication process. These MCs exhibited high CO_2 absorption performance and are expected to contribute to environmental impact reduction. However, they did not suppress carbonation in the mortar, raising concerns about the risk of reinforcement corrosion in structures.

It should be noted that the amine compounds encapsulated in this study were limited to DEA, TEA, MEA, and TOA, and the effectiveness of other amines remains to be verified.

Future research should focus on incorporating oil-soluble amine compounds with high CO_2 absorption capacities into mortars and evaluating the balance between strength development and CO_2 uptake. In addition, the potential of these MCs to exhibit corrosion-inhibiting effects and achieve multifunctionality should be investigated.

In conclusion, functional concrete utilizing MC technology is expected to contribute to the development of environmentally friendly concrete technologies and toward a more sustainable society. Furthermore, by modifying the core materials of MCs, diverse functionalities could be imparted to concrete, which may provide solutions to the wide range of challenges in infrastructure maintenance.

Supplementary Materials: Not applicable.

Author Contributions: Conceptualization, R.Y. and K.Y.; methodology, R.Y., R.K., K.I., S.K. and K.Y.; validation, R.Y., R.K., K.I., S.K. and K.Y.; investigation, R.Y. and K.Y.; resources, R.K., K.I. and S.K.; data curation, R.Y. and K.Y.; writing—original draft preparation, R.Y. and K.Y.; writing—review and editing, R.Y. and S.K.; visualization, R.Y. and K.Y.; supervision, S.K. and K.Y.; project administration, K.Y.; funding acquisition, R.K., K.I., S.K. and K.Y. All authors have read and agreed to the published version of the manuscript.

Funding: This research received no external funding.

Institutional Review Board Statement: Not applicable.

Informed Consent Statement: Not applicable.

Data Availability Statement: The datasets generated and/or analyzed during the current study are available from the corresponding authors upon reasonable request.

Acknowledgments: We would like to express our sincere gratitude to Prof. Koichiro Shiomori and Ms. Rika Fujimoto of the University of Miyazaki for their valuable support in the preparation and evaluation of the microcapsules using the in-liquid drying method.

Conflicts of Interest: Authors Ryusei Kondo and Koji Ishimaru are employed by the Kyokuto Kowa Corporation. The remaining authors declare that the research was conducted in the absence of any commercial or financial relationships that could be construed as a potential conflict of interest.

Abbreviations

The following abbreviations are used in this manuscript:

MC	Microcapsule
ASR	Alkali-silica reaction
MEA	Monoethanolamine (C_2H_7NO)
DEA	Diethanolamine ($C_4H_{11}NO_2$)
TEA	Triethanolamine ($C_6H_{15}NO_3$)
TIPA	Triisopropanolamine ($C_9H_{21}NO_3$)
TOA	Trioctylamine ($C_{24}H_{51}N$)
C-S-H	Calcium silicate hydrate
RC	Reinforced concrete
PL	Plain mortar without MC addition
MC-0	Mortar with MCs containing no TOA
MC-TOA	Mortar with MCs impregnated with 10% TOA by weight
TIPA	Triisopropanolamine ($C_9H_{21}NO_3$)
DEIPA	Di-ethanol isopropanolamine ($C_7H_{17}NO_3$)
MDEA	Methyl di-ethanolamine ($C_5H_{13}NO_2$)
SARS	Severe acute respiratory syndrome
MERS	Middle east respiratory syndrome
COVID-19	Coronavirus disease 2019

doi:10.20944/preprints202602.0063.v1

References

1. Takahashi, Y.; Jinnai, H.; Kubota, H.; Namiki, S.; Kuroiwa, S. Fundamental study on carbonation suppression effect for concrete by water-based finishing material. *AIJ Int. J. Technol. Des.* **2022**. (in Japanese), *28*, 545–549. DOI: 10.3130/aijt.28.545.
2. Liu, J.; Ruan, H.; Lu, B.; Chen, Z.; Shi, C. A new enhanced carbonation curing method using monoethanolamine (MEA) solution: Their effects on hydration and microstructure of cement-based materials. *Constr. Build. Mater.* **2023**, *396*, 132172. DOI: 10.1016/j.conbuildmat.2023.132172.
3. Xie, H.; Liu, X.; Zheng, Y.; Chi, B.; Guo, J.; Dai, X.; Zhang, Z.; Sun, M.; Duan, L.; Wang, Z.; Cui, S. Effect of complexation of alkanolamine in accelerators on the initial stage of cement hydration. *Constr. Build. Mater.* **2023**, *393*, 132105. DOI: 10.1016/j.conbuildmat.2023.132105.
4. Jiang, J.; Ye, Z.; Wu, J.; Yang, Q.; Li, Q.; Kong, X. Impact of triethanolamine on the hydration of Portland cement in the presence of high pozzolanic activity supplementary cementitious materials. *Cem. Concr. Compos.* **2024**, *147*, 105435. DOI: 10.1016/j.cemconcomp.2024.105435.
5. He, Y.; Liu, S.; Zhang, X.; Liu, W.; Liao, G.; Xu, M. Influence of triethanolamine on mechanical strength and hydration performance of blended cement containing fly ash, limestone and slag. *J. Build. Eng.* **2021**, *44*, 102879. DOI: 10.1016/j.jobe.2021.102879.
6. Zou, F.; Tan, H.; He, X.; Ma, B.; Deng, X.; Zhang, T.; Mei, J.; Liu, X.; Qi, H. Effect of triisopropanolamine on compressive strength and hydration of steaming-cured cement-fly ash paste. *Constr. Build. Mater.* **2018**, *192*, 836–845. DOI: 10.1016/j.conbuildmat.2018.10.087.
7. Zhao, Y.; Zhao, J.; Zhang, Y.; Qiu, C.; Zhang, H.; Yang, J. Cell membrane-inspired regulation of reactant diffusion for active agent microencapsulation via interface engineering. *Chem. Eng. J.* **2024**, *492*, 152311. DOI: 10.1016/j.cej.2024.152311.
8. Han, S.H.; Jun, Y.; Kim, J.H. The use of monoethanolamine CO_2 solvent for the CO_2 curing of cement-based materials. *Sustain. Mater. Technol.* **2023**, *35*, e00559. DOI: 10.1016/j.susmat.2022.e00559.
9. Li, L.; Yu, H.; Puxty, G.; Zhou, S.; Conway, W.; Feron, P. Integrated CO_2 capture and mineralization based on monoethanolamine and lime kiln dust. *Ind. Eng. Chem. Res.* **2024**, *63*, 16019–16028. DOI: 10.1021/acs.iecr.4c02064.
10. Rezania, M.; Moradnezhad, H.; Panahandeh, M.; Rahimpoor Kami, M.J.R.; Rahmani, A.; Hosseini, B.V. Effects of diethanolamine (DEA) and glass fibre reinforced polymer (GFRP) on setting time and mechanical properties of shotcrete. *J. Build. Eng.* **2020**, *31*, 101343. DOI: 10.1016/j.jobe.2020.101343.
11. Xin, P.; Liu, H.; Wang, J.; Wang, Y.; Wang, H.; Cui, S. Effects of CO_2-absorbed triethanolamine solutions on strength development of cement mortars and the mechanism: Synergism of cement hydration and carbonation. *Constr. Build. Mater.* **2024**, *413*, 134708. DOI: 10.1016/j.conbuildmat.2023.134708.
12. Song, H.; Atarashi, D.; Hosokawa, Y.; Miyawaka, M. *Effect of Alkanolamine on Early Hydration Reaction of Fly Ash Cement, Cement Science and Concrete Technology*. 2020. (in Japanese), 73, 59–64.
13. Zhang, T.; Sun, Z.; Yang, H.; Ji, Y.; Yan, Z. Enhancement of triisopropanolamine on the compressive strength development of cement paste incorporated with high content of wasted clay brick powder and its working mechanism. *Constr. Build. Mater.* **2021**, *302*, 124052. DOI: 10.1016/j.conbuildmat.2021.124052.
14. Zhou, J.; Jia, Y.; Wei, C.; Li, W.; Liu, Y. Reactive extraction of methanesulfonic acid from wastewater using trioctylamine, *Sci. Rep.* **2024**, *14*, 30029. DOI: 10.1038/s41598-024-81916-8.
15. Li, W.; Luo, T.; Zhu, C.; Xu, D.; Dong, Y.; Cao, B. Facile synthesis of lipophilic alkylated boron nitride nanosheets as lubricating oil additive to greatly enhance the friction and heat-conducting properties. *Tribol. Int.* **2022**, *173*, 107655. DOI: 10.1016/j.triboint.2022.107655.
16. Karnwiboon, K.; Krajangpit, W.; Supap, T.; Muchan, P.; Saiwan, C.; Idem, R.; Koiwanit, J. Solvent extraction based reclaiming technique for the removal of heat stable salts (HSS) and neutral degradation products from amines used during the capture of carbon dioxide (CO_2) from industrial flue gases. *Sep. Purif. Technol.* **2019**, *228*, 115744. DOI: 10.1016/j.seppur.2019.115744.
17. Henczka, M.; Dja M. Reactive extraction of acetic acid and propionic acid using supercritical carbon dioxide. *J. Supercrit. Fluids*, **2016**, *110*, 154-160. DOI: 10.1016/j.supflu.2015.11.018.
18. Tanaka, M. Microcapsules. *J. Jpn Soc. Colour Mater.* **1998**. (in Japanese), *71*, 593–598. DOI: 10.4011/shikizai1937.71.593.

doi:10.20944/preprints202602.0063.v1

19. Ozban, G.; Franco, P.; Marco, D.; Xiao, J.; Capanoglu, E. A review of microencapsulation methods for food antioxidants: Principles, advantages, drawbacks and applications. *Food Chem*. **2019**, *272*, 494–506. DOI: 10.1016/j.foodchem.2018.07.205.
20. Choudhury, N.; Meghwal, M.; Das, K. Microencapsulation: An overview on concepts, methods, properties and applications in foods. *Food Front*. **2021**, *2*, 4, 426-442. DOI: 10.1002/fft2.94.
21. Minami, M.; Tsuji, S.; Akagawa, S.; Kaneko, K. Development of Gut Microbiota in Childhood: Focusing on the effects of mode of delivery and nutrition in neonatal period. *J. Kansai Med. Univ.* **2025**. (in Japanese), *76*, 35–40. DOI: 10.5361/jkmu.71.7.
22. Shiomori, K. Preparation of microcapsules and microparticles and their application to extraction and separation. *Abstr. Ion Exch. Semin*. **2023**. (in Japanese), *35*, 12–21.
23. Litina, C.; Al-Tabbaa, A.A. First generation microcapsule-based self-healing cementitious construction repair materials. *Constr. Build. Mater.* **2020**, *255*, 119389. DOI: 10.1016/j.conbuildmat.2020.119389.
24. Mao, H.; Cao, X.; Guo, M.; Jiang, C.; Chen, D. Study on the repair effect of self-healing cementitious material with urea-formaldehyde resin/epoxy resin microcapsule. *Buildings* **2024**, *14*, 2201. DOI: 10.3390/buildings14072201.
25. Xing, X.; Zhong, G.; Wu, Z.; Cai, J.; Cheng, X. Self-healing mechanism of deposited carbonates in cement cracks under CO_2 storage well conditions. *Front. Mater.* **2022**, *9*, 1013545. DOI: 10.3389/fmats.2022.1013545.
26. Kawano, Y.; Hatate, Y. Preparation and control of microcapsules. *J. Soc. Powder Technolo. Japan* **2003**. (in Japanese), *40*, 736–745. DOI: 10.4164/sptj.40.736.
27. Makino, K. Chemistry of microcapsules, Oreo science **2001**. (in Japanese), *1*, 25–30.
28. Japanese Standards Association. JIS A. *Test Method Compressive Strength Concr.* **2019**. (in Japanese), *1108*.
29. Japanese Standards Association. JIS A. *Test Method Accel. Carbonation Concr*. **2012**. (in Japanese), *1153*.
30. Fukushima, M.; Uesugi, K.; Hirose, Y.; Ohzuno, Y.; Shiomori, K.; Kiyoyama, S.; Takei, T.; Yoshida, M. Preparation of melamine-formaldehyde microcapsules incorporating reactive monomer for self-healing. *Stud. Sci. Technol*. **2014**. (in Japanese), *3*, 127–132.
31. Shiomori, K.; Kawano, Y.; Kiyoyama, S.; Yoshida, M.; Hatate, Y. Structural control of microcapsules prepared by in situ polymerization. *Powder Sci. Eng.* **2005**. (in Japanese), *37*, 37–46.
32. Laribi, S.; Dubois, L.; Weireld, G.D.; Thomas, D. Study of the post-combustion CO_2 capture process by absorption-regeneration using amine solvents applied to cement plant flue gases with high CO_2 contents. *Int. J. Greenh. Gas Control*. **2019**, *90*, 102799.
33. Hanifa, M.; Agarwal, R.; Sharma, U.; Thapliyal, P.C.; Singh, L.P. A review on CO_2 capture and sequestration in the construction industry: Emerging approaches and commercialised technologies. *J. CO_2 Util.* **2023**, *67*, 102292. DOI: 10.1016/j.jcou.2022.102292.
34. Fernandes, D.; Conway, W.; Burns, R.; Lawrance, G.; Maeder, M.; Puxty, G. Investigations of primary and secondary amine carbamate stability by ^{1}H NMR spectroscopy for post combustion capture of carbon dioxide. *J. Chem. Thermodyn.* **2012**, *54*, 183–191. DOI: 10.1016/j.jct.2012.03.030.
35. Mannisto, J.K.; Pavlovic, L.; Tiainen, T.; Nieger, M.; Sahari, A.; Hopmann, K.H.; Repo, T. Mechanistic insights into carbamate formation from CO_2 and amines: The role of guanidine–CO_2 adducts. *Catal. Sci. Technol*. **2021**, *11*, 6877–6886. DOI: 10.1039/D1CY01433A.
36. Shiomori, K.; Kiyoyama, S.; Takei, T.; Yoshida, M. Separation technology using extractant-encapsulated microcapsules. In Symposium Series 2: Practical Applications of Separation Seeds and Licensed Technologies (in Japanese), The Society of Separation Process Engineers: Tokyo, Japan. 2018; pp. 54–60.
37. Zhang, X.; Li, J.A.; Kang, J.; Yu, S.; Gao, Z.; Gou, J.; Yu, B. Amine-based microcapsules for recyclable CO_2 capture with high stability. *Results Eng*. **2019**, *27*, 106788. DOI: 10.1016/j.rineng.2025.106788.
38. Solangi, N.H.; Hussin, F.; Anjum, A.; Sabzoi, N.; Mazari, S.A.; Mubarak, N.M.; Aroua, M.K.; Siddiqui, M.T.H.; Qureshi, S.S. A review of encapsulated ionic liquids for CO_2 capture. *J. Mol. Liq*. **2023**, *374*, 121266. DOI: 10.1016/j.molliq.2023.121266.
39. Shiomori, K.; Kiyoyama, S. Micro/nanocapsules containing extractant for metal ion extraction (in Japanese). *Energy Resour*. **2016**, *37*, 5, 306–311.

40. Kumar, R.; Bandyopadhyay, M.; Pandey, M.; Tsunoji, N. Amine-impregnated nanoarchitectonics of mesoporous silica for capturing dry and humid 400 ppm carbon dioxide: A comparative study. *Microporous and Mesoporous Mater.* **2022**, *338*, 111956. DOI: 10.1016/j.micromeso.2022.111956.
41. Sami, A.; Rabat, N.E.; Johari, K.; Shamsuddin, M.R.; Chani, S.M.M.; Ghumman, A.S.M.; Khan, M.S. Development of an amine-impregnated polymer aerogel for CO_2 capture. *Colloids Surf. A.* **2024**, *690*, 133778. DOI: 10.1016/j.colsurfa.2024.133778.
42. Wang, E.; Luo, L.; Wang, J.; Dai, J.; Li, S.; Chen, L.; Li, J. A dataset for investigations of amine-impregnated solid adsorbent for direct air capture. *Sci. Data* **2025**, *12*, 724. DOI: 10.1038/s41597-025-05037-1.
43. Hack, J.; Maeda, N.; Meier, D.M. Review on CO_2 capture using amine-functionalized materials. *ACS Omega* **2022**, *7*, 44. DOI: 10.1021/acsomega.2c03385.
44. Wang, Y.; Marreiros, J.; Thompson, J.A.; Toops, T.J.; Campbell, Z.S.; Kidder, M.K.; Janke, C.J.; Leow, J.Q.; Sholl, D.S.; Lively, R.P. Performance degradation of amine-infused fiber sorbents for direct air capture: Mechanisms and solutions. *Ind. Eng. Chem. Res.* **2025**, *64*, 26. DOI: 10.1021/acs.iecr.5c00462.
45. Priyadarshini, P.; Rim. G.; Rosu, C.; Song, MG.; Jones, C.W. Direct air capture of CO_2 using amine/alumina sorbents at cold temperature. *ACS Environ. Au* **2023**, *3*, 5, 295–307. DOI: 10.1021/acsenvironau.3c00010.
46. Wang, E.; Luo, L.; Wang, J.; Dai, J.; Li, S.; Chen, L.; Li, J. A dataset for investigations of amine-impregnated solid adsorbent for direct air capture. *Sci. Data* **2025**, *12*, 724. DOI: 10.1038/s41597-025-05037-1.
47. Japanese Standards Association. JIS. *Gen. Rules Determination Carbon Metallic Mater.* **2015**. (in Japanese), *Z2615*.
48. Jawahar, J.; Vishnudas, S. Enhanced mechanical strength and permeability in Portland pozzolana cement through optimized self-healing microcapsule dosage. *Innov. Infrastruct. Solut.* **2025**, *10*, 202. DOI: 10.1007/s41062-025-02008-8.